International Journal on Magnetic Particle Imaging
Vol 6, No 2, Suppl 1, Article ID 2009047, 3 Pages

Infinite Science Publishing

Proceedings Article

Simulation study to minimize the dimensions of a single-sided FFP MPI scanner

K. Gräfe[1,*] · T. M. Buzug[1]

[1]Institute of Medical Engineering, University of Lübeck, Lübeck, Germany
[*]Corresponding author, email: graefe@imt.uni-luebeck.de

Abstract

One medical application scenario of a single-sided field free point (FFP) magnetic particle imaging (MPI) scanner is the localization of sentinel lymph nodes of patients with breast cancer. For this clinical application, the minimization of the scanner is essential to enable a comfortable patient access. Existing single-sided MPI scanners are non-flexible systems with limited field of view. This abstract presents a simulation study of a flexible downscaled single-sided FFP MPI scanner with unconfined field of view.

I Introduction

The single-sided FFP MPI scanner presented in [1] is a static installed system with a maximum diameter of 140 mm. For clinical applications, the localization of the sentinel lymph node in the case of breast cancer, it is desirable to reduce the size of this system to make it compact and movable, and that the dimensions of the system fit to the human axilla. To realize this, a maximum diameter of the scanner device of 100 mm is preferable.

This abstract discusses the idea of using permanent magnets to make the device more compact. With permanent magnets generating the gradient field, it will be possible to build up the MPI scanner without a complicated cooling concept. This abstract presents a simulation study.

II Material and methods

For the simulation study, the simulation software ScannerConf, developed at the Institute of Medical Engineering [2], was used. This software allows the calculation and display of magnetic fields considering different geometries of permanent magnets and coils and the assignment of further different characteristics. In addition, it is possible to display the FFPs and the trajectories on which the FFPs move.

Two circular permanent magnets generate the selection field. Due to their nested arrangement, one FFP is generated on both sides of the permanent magnet assembly. In this study, both FFPs are considered. Thus, two different magnetic fields and trajectories can be realized. This allows the downscaling of the single-sided scanner without further limitations of the FOV size. Additional to the permanent magnets coils are necessary, which are carrying an alternating current and generate the excitation fields. At this early stage of the simulation, the same excitation frequencies as in [1] are used for the one-dimensional and two-dimensional excitation. Thus, the FFPs move along two different Lissajous trajectories. Table 1 summarizes the most important specifications of the simulated setup. For the selection of the permanent magnets, it was taken into account that their remanence density Br and the surface current I_0 are in the order of commercially available permanent magnets. B_r indicates the flux density, if no external field is active and can be read in the hysteresis curve at the point H = 0. The surface current I_0 comes about because permanent magnets can be modeled by homogeneously distributed

Table 1: The geometry properties and specifications of the coils and the permanent magnets [3].

	outer permanent magnet	inner permanent magnet	coil for the FFP movement in x-direction	coil for the FFP movement in y-direction
form	circular	circular	circular	double D-shaped
outer radius	50 mm	40 mm	25 mm	50 mm
inner radius	44 mm	25.5 mm	5.5 mm	37 mm
high	15.5 mm	15.5 mm	15.5 mm	4.5 mm
surface current	310.35 MA/m	103.85 MA/m	-	-
number of turns	-	-	36	8
alternating current	-	-	83 A	160 A
power loss	-	-	51.72 W	93.44 W
frequency	-	-	2.5 MHz/99	2.5 MHz/96

dipole moments and can be calculated by

$$I_0 \frac{B_r}{\mu_0}, \tag{1}$$

with $\mu_0 = 4\pi 10^{-7} \mathrm{NA}^{-2}$. Due to this distribution, the volume flow is extinguished in favor of the surface current. The chosen field of view (FOV) size is 30 mm x 30 mm. For the simulation, the FOV is positioned directly above the simulated scanner setup on each size of the permanent magnets.

To evaluate the simulation setup the magnetic flux density, the gradient and the courses of the FFPs are simulated. For reasons of comparability, the same phantom used in an earlier study [4] was used again to simulate the imaging process. For reconstruction, the resolution of the FOV is 15 x 15 points and 50 iterations of the algebraic reconstruction technique were calculated. The L-curve based regularization parameter is $\lambda = 10^{-18}$.

III Results and discussion

In figure 1 on the left side, an exploded view of the simulation setup is shown. On the right side, the simulation setup and the different FOVs are shown. The FOVs and the trajectories, on which the FFPs are moved, differ from each other, depending on which side of the setup the FFP is viewed.

Figure 2 shows the selection field on each size of the simulation setup. In figure 3, the simulated reconstruction results of the phantom (fig. 3a) on each side of the simulation setup (compare fig.1) are shown. In fig. 3b the reconstruction results of the phantom which was placed directly above the circular coil is shown and fig. 3c shows the reconstruction result, if the phantom is placed directly above the D-shaped coils.

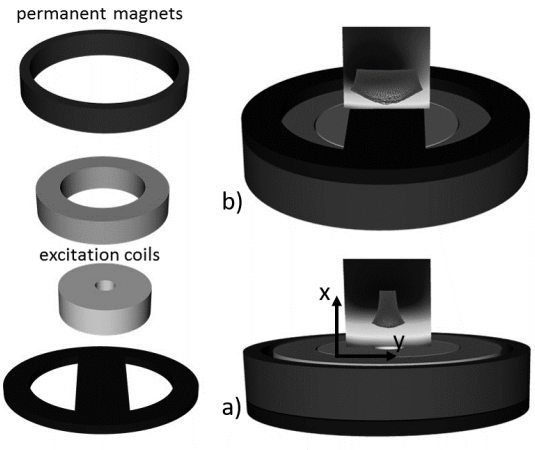

Figure 1: The left side shows the individual geometries of the simulation setup as an exploded view. On the right side, the whole simulation setup is illustrated. Additionally, the FOV and the trajectories of the FFPs on each size of the simulation setup are shown [3].

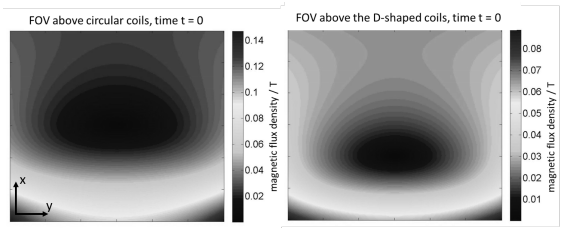

Figure 2: The magnetic flux density of the selection field above the circular coil (left) and above the D-Shaped coils (right).

IV Discussion and Conclusion

Because the FFPs on both sides of the setup are used for the imaging process, two different trajectories are generated (fig. 1). Figure 2 shows, that the FFP position is depending on which side of the setup the FOV is positioned. The effect is that on one side of the scanner it will be possible to locate particles that are about 19 mm apart from the scanner surface (fig. 3b). In contrast, to this, on the other side of the scanner only particles can be located which are positioned in the direct neighborhood of the scanner surface, (fig. 3c).

With this simulation study, it is possible to show the possibility of a smaller and thus more versatile single-sided MPI scanner. For the realization step, further calculations must be carried out to improve the concept.

Acknowledgments

The authors would like to thank C. Debbeler for the proofreading.

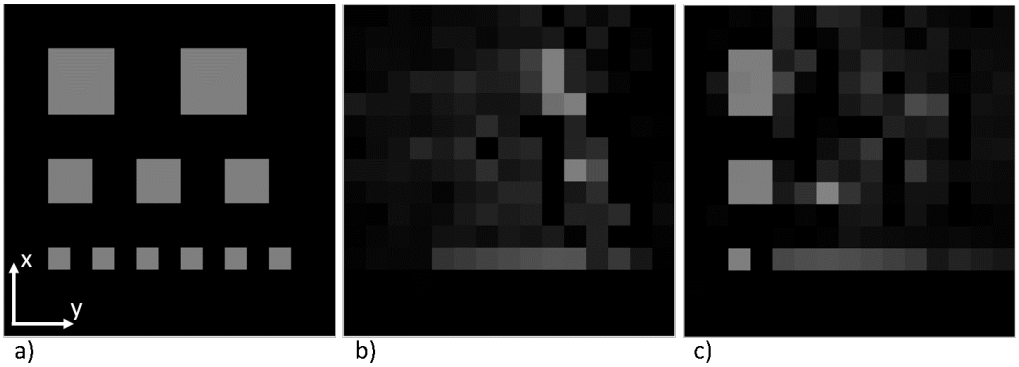

Figure 3: The normalized reconstruction results of a 30 mm x 30 mm resolution phantom (a), which was positioned on both sides of the scanner. The scanner is located on the bottom of each phantom. b) shows the reconstruction result of the phantom, which was placed above the circular coil (Fig. 1a). c) shows the reconstruction result of the phantom placed above the D-coils (Fig. 1b) [3].

Author's Statement

Research funding: The authors state no funding involved.
Conflict of interest: Authors state no conflict of interest.

References

[1] K. Gräfe et al., 2D Images Recorded with a Single-Sided Magnetic Particle Imaging Scanner. IEEE Trans. Med. Imag., 35(4):1056-1065, 2016. doi: 10.1109/TMI.2015.2507187.

[2] T. Knopp, Effiziente Rekonstruktion und alternative Spulentopologien für Magnetic-Particle-Imaging. SpringerVieweg, Heidelberg, 2011.

[3] K. Gräfe, Bildgebungskonzepte für Magnetic Particle Imaging - Magnetic Particle Imaging mit einer asymmetrischen Spulentopologie. Infinite Science Publishing, Lübeck, 2016.

[4] K. Gräfe et al., Phantom simulation based on measured gradient fields of a single-sided MPI scanner. IWMPI, 2013, doi: 10.1109/IWMPI.2013.6528352.

